

**Recognition of rayed craters on Mars using day and nighttime temperature images from the Mars Odyssey's Thermal Emission Imaging System (THEMIS).** L. L. Tornabene<sup>1\*</sup>, J. Piatek<sup>1</sup>, J. E. Moersch<sup>1</sup> H. Y. McSween Jr.<sup>1</sup> and P. R. Christensen<sup>2</sup>, <sup>1</sup>Department of Earth and Planetary Sciences, University of Tennessee, Knoxville, Tennessee 37996-1410, USA, <sup>2</sup>Department of Geological Sciences, Arizona State University, Tempe, Arizona 85287-6305, USA.

**Introduction:** Four new rayed craters have been identified on Mars using images from the Mars Odyssey Thermal Infrared Imaging System (THEMIS). Similar to the rayed crater Zunil, discovered by McEwen et al. [1-3], these craters are easily recognizable in THEMIS nighttime (nTIR) and daytime (dTIR) thermal infrared images. From these 5 examples it has been observed that Martian crater rays are nearly undetectable in visible wavelength imagery, unlike lunar, Mercurian, and Galilean satellite rayed craters, which are well known for a distinctive albedo contrast with the surface materials they superimpose. However, Martian crater rays are also recognized by a contrast, but in brightness temperature ( $T_B$ ) rather than by a contrast in albedo (compare Fig. 1A with 1B). The recognition of unique thermophysical units for one Martian rayed crater has enabled the identification of additional rayed craters by surveying a global mosaic of THEMIS nTIR and dTIR imagery.

**Methods and Results:** A global THEMIS nTIR mosaic was surveyed from 45N to 45S using JMars (a program developed by ASU that overlays various Martian datasets [4]). In addition to Zunil (located at 166E 7.7N) [1-3], four rayed craters have been recognized: \*A, B, C and D (\*- names are currently being considered for submission to IAU). Once these crater ray systems were recognized in the THEMIS imagery, overlays of other datasets (e.g. MOC, THEMIS VIS, MDIM, TES-thermal inertia) were applied in JMars to observe and describe rayed crater characteristics with respect to observations made in the nTIR and dTIR images.

**General observations:** Martian rayed craters can be identified by their very distinct temperature facies in THEMIS nTIR images (see Fig. 1). They are easily recognizable in examples where at least a small portion of the ray system has a contrasting  $T_B$  to the surrounding area. Martian rays are visible in TIR images only where there is a significant temperature contrast (e.g. at night, if a surface is also cool then one cannot see the cool rays superimposed on it). This was the case with Zunil, which has many of its rays deposited over a background material with a similar thermophysical signature, and therefore many of its rays are indistinguishable from the background temperature in TIR images. [see Fig. 7 in 3].

Table 1. summarizes characteristics of each of the crater ray systems discovered thus far on Mars.

**Table 1. Martian rayed crater characteristics**

Name	D (km)	Rays <sup>2</sup> #	(km) Length	(km) Width (max) <sup>2</sup>
A	6.9 <sup>1</sup>	>20	~540	2-8 (13.8)
B	~3.3 <sup>2</sup>	7	~200	1-2 (3)
C	7.4 <sup>1</sup>	9	540-600	2-5 (6.5)
D	~2.0 <sup>2</sup>	4	40-50	1-1.5 (2.7)
Zunil	10.1 <sup>3</sup>	5	~800 <sup>3</sup>	1-4 (6.5)

<sup>1</sup>Mars Crater Database [5]

<sup>2</sup>Measured in nTIR images using JMars (MOLA DEM overlay)

<sup>3</sup>from McEwen et al. [1-3].

Crater A has the largest number of distinguishable rays, which is more than double that of any of the other rayed craters. Maximum ray lengths range from 25-81 times the diameter of the source crater, with Zunil having the longest recognizable rays in nTIR images and Crater C having the highest length to diameter ratio. Unlike lunar crater rays, which have ray widths that are consistently comparable to the source crater radius [7], Martian ray widths range from a minimum of 0.5 to 2.0D (compare Fig. 1E and D), with the average ray being 0.95D in width.

**Ray Morphology.** Martian rays are composed of feathery and arcuate en echelon elements radial to subradial to the source crater (Fig. 1). As observed at Zunil [1-3], and similar to rayed craters on other bodies, high resolution visible imagery from THEMIS (~18m/pixel) and MOC (~5m/pixel) indicate that they are comprised of numerous, densely and narrowly clustered small (generally, <100 m) secondary impact craters. Many of these small secondary impacts have dark interiors and overlapping ejecta blankets consisting of a darker facies with an outer lighter toned facies. These ejecta materials appear to represent the predominant material that makes up the dark rays seen in the nTIR.

**Thermophysical units.**  $T_B$  can be used as a proxy for thermal inertia (TI) within a given THEMIS nTIR scene. Different thermophysical units, defined here, are likely to arise from differences in grain size, with darker "cooler" areas having lower TI and smaller grain size, and brighter "warmer" areas having higher TI and larger grain sizes [8]. Of all the rayed craters discovered so far, Crater A is the largest and most complete rayed crater viewable in THEMIS nTIR imagery. For Crater A, 6 thermophysical units can be defined in nTIR imagery along the radial direction

outward from the crater (see Fig. 1D for Units 1-5 and Fig. 1E for Unit 6). “High” and “low” thermal inertias in the following thermophysical facies description are meant in a relative sense:

*Crater units:*

1. Low TI intra-crater deposits
2. High TI Crater wall/rim (possible exposed bedrock)

*Ejecta units:*

3. Low TI continuous ejecta blanket (appears to be associated w/ a small fluidized ejecta blanket)
4. High TI continuous ejecta blanket (subsurface ejecta materials – exposed bedrock)
5. Low TI continuous ejecta (dust?)

*Ray unit:*

6. Predominantly low TI rays sometimes w/ higher TI cores

In addition to 100m/ pixel THEMIS images, Martian rayed craters can also be recognized in the coarser resolution (~5 km/pixel) Thermal Emission Spectrometer (TES) dataset. Rayed craters have a distinct thermophysical signature in thermal inertia maps generated from TES data, with individual rays being detectable in some cases (Fig. 1C). A concentric pattern can be recognized in the TES derived TI maps for 3 of the 5 Martian rayed craters. The concentric pattern is consistent with units 4-6 defined above, with dashed concentric circles in Fig. 1C representing the approximate boundaries of these 3 units. The inner circle exhibits relatively high TI values (light blue) consistent with unit 4, while the circle surrounding the center (mostly purple) corresponds to unit 5. The outermost circle (mostly blue) is consistent with unit 6, a mixture individual “cooler” rays and the warmer surroundings. Craters A, B and C have this signature, but D and Zunil do not, possibly because D is too small to be seen with the coarser TES pixel and Zunil occurs predominantly within a cold, “dust-covered” region.

With the exception of Zunil, all of the Martian rayed craters presented here have ejecta patterns consistent with low angle impacts (20-45°). This is based on the presence of a forbidden zone (Fig.1C), a wedge-shaped zone devoid of ejecta typically forming up range from the travel direction of the impactor [8]. The forbidden zone can be seen in THEMIS imagery, but can be most easily discerned in the TES-derived TI image as a light-blue wedge SSW of the center (outlined by a solid line).

*Atmospheric and weathering effects.* The presence of rayed crater systems on Mars debunks existing ray formation models that assume that rayed crater systems only form on airless bodies [9]. However,

the presence of a thin atmosphere on Mars appears to have an effect on the formation of distant ray elements. Atmospheric interactions may be suggested by the curved ray morphology of Crater C. One explanation for curved rays is that they may form due to a Coriolis Effect acting on high altitude ejecta as it resettles through the Martian atmosphere [10]. Why only crater C shows curved ray elements and the others do not is not understood. Further in-depth studies of these craters will be necessary to better understand the formation mechanisms involved. The rarity of rayed craters on Mars may provide insight into the rate at which current environmental conditions can erase thermophysical signatures on the surface.

**Conclusions:** Martian rayed craters are readily identified in nTIR and dTIR images from THEMIS and can even be recognized in TES datasets despite the coarser resolution of 3x6km/pixel. There appears to be only a weak albedo contrast between ray material and the surface materials they overlie, which has confounded the identification of rayed craters in datasets previous to THEMIS. Martian rayed craters appear to be most easily recognized if there is a thermal contrast between the ray materials and the background surface they superimpose. To date, THEMIS offers the best views of these features. In the absence of thermally contrasting units, a rigorous study of secondary crater chains, such as that of McEwen et al. [1-3], would be necessary to positively identify other Martian rayed craters.

**Future Work:** We are working towards retrieving quantitative thermal inertias and performing a full spectral/compositional analysis of the units defined here using the THEMIS image database. Corrections for slope effects and atmospheric dust opacity, which affect  $T_B$ , are necessary for accurate quantitative results necessary for this work. Rays that are wide enough will be spectrally analyzed with TES data to determine whether there is a compositional or particle size contrast with the surrounding surface materials. Better coverage by THEMIS and MOC images of the craters presented here will be requested in order to better constrain the nature of rayed craters. An anticipated and more complete THEMIS dTIR global mosaic will also be searched for additional rayed craters that may have been missed in the nTIR.

**References:** [1] McEwen et al. (2003) *LPS XXXIV*, Abstract #2040. [2] McEwen A. S. (2003) *6<sup>th</sup> Inetrnat. conf. Mars*, Abstract #3268. [3] McEwen et al. (in review) *Icarus*. [4] Gorelick et al. (2003) *LPS XXXIV*, Abstract #2057. [5] Barlow N. G. (2003) *6<sup>th</sup> Inetrnat. conf. Mars*, Abstract #3073. [7] Hawke B. R. et al. (2004) *Icarus*, 170, 1-16. [8] Mellon et al. (2000) *Icarus*, 148, 437-455. [9] Melosh H. J. (1989) *Impact Cratering*, 245 pp. [10] Wrobel K. E. and Shultz P. H. (2004), *JGR*, 109, E05005.

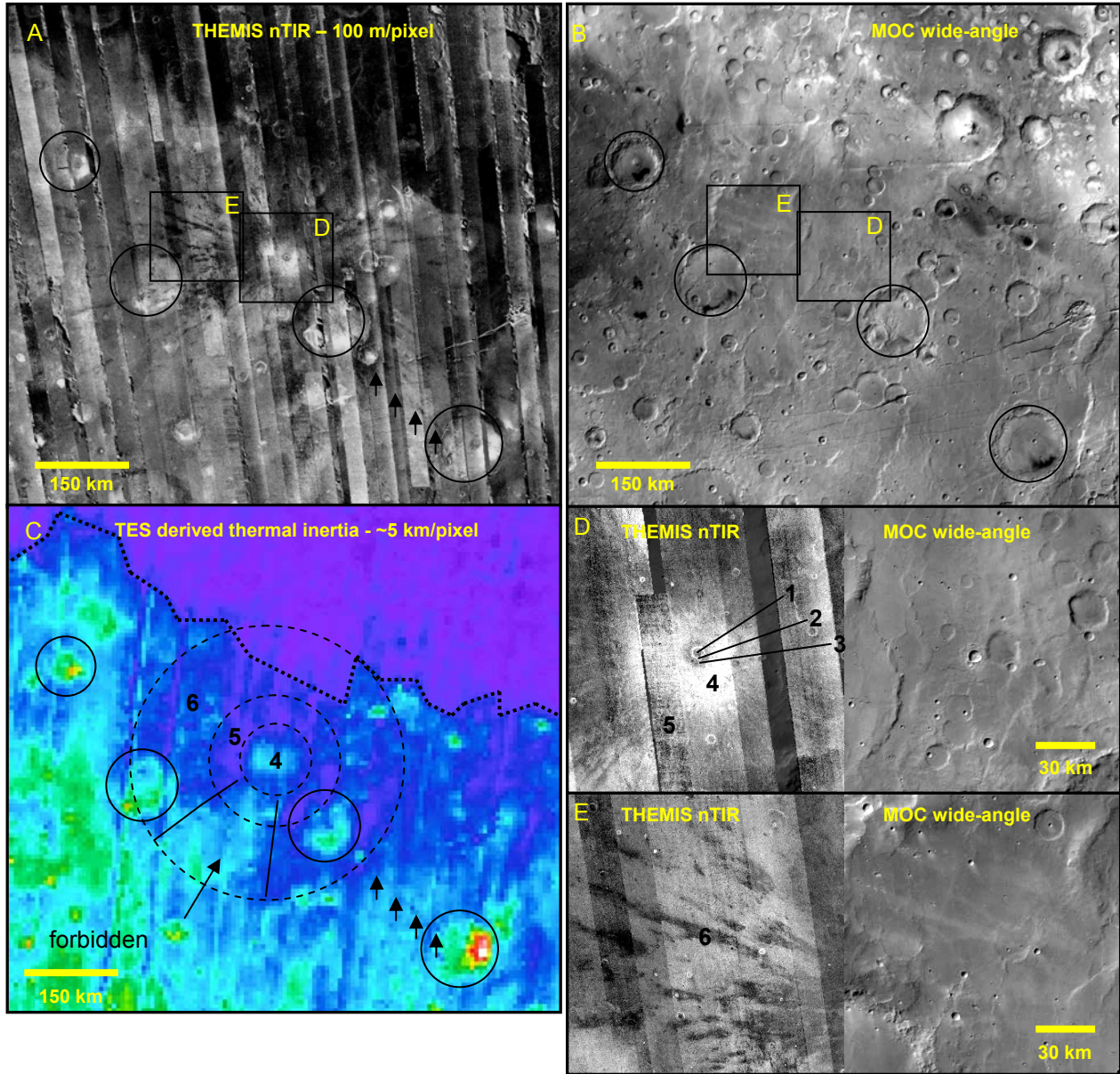


**Figure 1.** Images associated with Martian rayed crater A (north is up in all images). Images A, B and C are the same scale. The **upper left** image (A) is a mosaic of nTIR (brightness temperature) images. Cooler (dark) ray material is superimposed on a warmer (grays through white) surface. A dark region (colder) lying to the north is likely dust-covered. The **upper right** image (B) is a panchromatic, wide-angle camera MOC image of the same area as seen in the upper right. The rays easily seen in image A as thermophysical features are barely discernable in a visible image (see E). The **bottom left** image (C) is a TES derived TI map which shows a concentric pattern consistent with Units 4-6. Craters are circled here and in other images. These craters are traps for high TI deposits. A detectable ray is outlined by arrows and corresponds to the dark ray outlined by the arrows in the upper left image. The dotted line approximates the contact between low TI area to the north and moderate to high TI to the south. The straight lines outline what is interpreted here as a forbidden zone, which suggests an oblique impact (20-45°). The **bottom right** images are blow ups of the outlined areas D and E from images A and B. The nTIR images D and E show the locations of Units 1-6.